VIBRATION CONTROL OF A SMART HELICOPTER BLADE

José Nilson Gasparini
gasparini2002@yahoo.com.br

Flávio Donizeti Marques
fmarques@sc.usp.br

School of Engineering of São Carlos – USP
Av. Trabalhador Sancarlense, 400
13566-590, São Carlos, SP

Abstract. *The objective of this work is to investigate the performance of a smart helicopter blade. Developments of smart materials for both sensing and/or actuation work provided a novel alternative in vibration control. The blade is modeled by the finite element method, considering the motions of flapping, lead lagging, axial stretching, and torsion. The blade model also considers a pretwist angle, offset between mass and elastic axes and isotropic material. A helicopter blade mathematical model is developed and it allows the incorporation of piezoelectric actuators distributed along the blade span. The active vibration control is based on the premise of individual blade control and the investigation is carried out for hovering flight condition The finite element matrices are obtained by energy methods and a linearization procedure is applied to the resulting expressions. The linearized aerodynamic loading is calculated for hover and the state-space approach is used to design the control system. The eigenstructure assignment by output feedback is used in the blade-reduced model resulting from the application of the expansion method by partial fractions. The simulations for open and closed-loop systems are presented, having exhibited good response qualities, what shows that output feedback is a good alternative for smart helicopter blade vibration attenuation.*

Keywords*. Aeroelasticity, vibration control, smart structures, eigenstructure assignment, helicopter blade modeling*

1. Introduction

Rotary wing aircraft are typically subjected to vibrations. The main source of these vibrations is the rotor, which is formed by flexible blades excited by periodical aerodynamic and inertial loads. These vibrations are transferred to the vehicle structure and usually create a hostile environment for other devices, crew, or even passengers. Significant amount of research work has been developed to look for solutions to the vibration problems, and considerable progress has already been reached.

Among the ways to reduce vibration problems in helicopters, the passive and active control could be mentioned. The former tries to control the helicopter oscillatory response through an accurate structural design, e.g., using optimization techniques or by installing devices in the rotor or fuselage in order to absorb, or isolate, the vibration sources (Reichert,1981; Loewy 1984). The later uses the techniques from automatic control systems. Friedmann (1990) presents a good view on the development of these techniques applied to helicopters.

The recent developments in smart materials have provided a promising framework to attaining automatic vibration control in helicopters. Smart materials exhibit induced-strain under the action of an electric or magnetic field. Most common smart or active materials are the piezoelectric, electro and magnetostrictive alloys, and the electro- and magneto-rheological fluids (Crawley, 1994). Helicopter applications of smart materials appear as a viable alternative in vibration control. Two methodologies for the application of smart materials have been investigated, that is: (1) distributed induced-strain actuators; (2) discrete actuation of a servo-aerodynamic control surface.

Induced blade twist by means of smart materials embedded in the structure has been investigated. A number of theoretical works have been developed to estimate the degree of twist required to affect flutter and vibration reduction benefits (Nitzsche and Breitbach, 1992; Nitzsche, 1994). Rotor blade flap actuation has been investigated as an alternative approach to achieving induced-strain rotor blade vibration attenuation. Theoretical studies have been performed and innovative concepts for servo-flaps presented (Millott and Friedmann, 1994).

From automatic control systems applied to helicopter vibration control, the modern control theory has been much used these days. Takahashi and Friedmann (1991) have considered the rotor-fuselage coupling model. Nguyen and Chopra (1990) consider only the rotor and the control is applied by exciting the blade with higher harmonics of the blade rotational speed, the so-called, higher harmonic control - HHC. The eigenstructure assignment technique is an alternative for control, where the eigenstructure of a desired closed-loop system and assessing gain matrices can be assigned. For helicopter vibration reduction this approach can be seen in Straub and Warmbrodt (1985) who used state feedback, but no other work using the eigenstructure assignment was found. The eigenstructure assignment technique makes possible to have a better insight of feedback gains assessment and it is more appropriate for multivariable systems.

The objective of this work is to investigate the application of piezoelectric actuators embedded in a helicopter blade structure to promote active control of vibrations. The helicopter blade is considered as a cantilever-rotating beam undergoing bending-torsion coupling motions. The finite element method has been used to model the hingeless blade, which had its order reduced by the method of expansion of partial fractions. Piezoelectric actuation and aerodynamic

loading are also incorporated to the model. The eigenstructure assignment by output feedback for vibration control of a helicopter blade is applied. The gain matrix has been calculated by the blade-reduced model using the output feedback. Assigned and achieved eigenvalues used for the control design have shown good agreement, assuring the success of the control law. Simulations of the open and closed-loop systems have also been presented and discussed.

2. Mathematical Modeling

The blade studied here is modeled as a rotating cantilever beam with length R, undergoing the coupling motions of flapping, lead-lagging, axial stretching and torsion and was based on Marques (1993). A pretwist angle θ_t is adopted in the model, considered null in the blade root and varying linearly through the span. It is also supposed that elastic and mass axes are noncoincidents.

The main coordinate systems of the blade model are shown in Figs. (1) and (2). Figure (1) shows the main coordinate system *x*, *y* and *z*, that is fixed in the blade root with its origin in the intersection of blade root cross-section and elastic axis. When the blade is not deformed the *x*-axis is exactly coincident with the elastic axis. Figure (1) also shows the deformed blade and elastic displacement u, v and w, in the x, y and z directions, respectively. Figure (2) shows an arbitrary blade cross-section and its local coordinate system η and ζ. The torsional deflection ϕ, due to the blade deformation can also be seen.

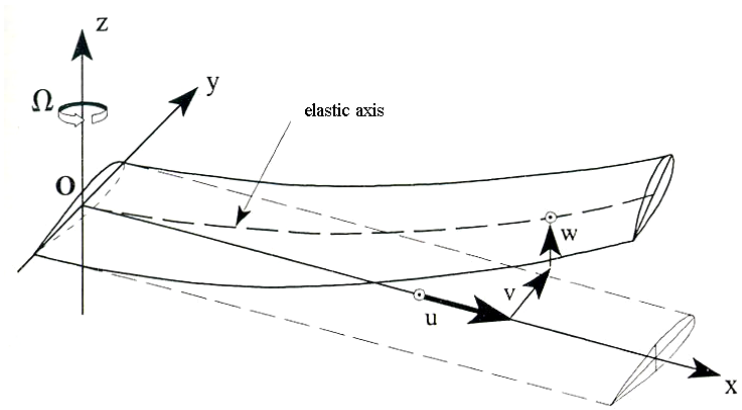

Figure 1 - Blade coordinate system and elastic displacement

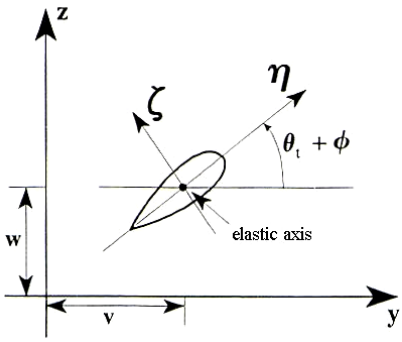

Figure 2 - Cross-sectional coordinate system

2.1. Strain and kinetic energy

The strain energy, considering a rotating beam undergoing axial stress, shear in the lead-lagging plane and in the flapping plane, is given by:

$$U = \frac{1}{2}\int_0^R \left\{ EAu'^2 + EI_z\left(v''\cos\theta_t + w''sin\theta_t\right)^2 + EI_y\left(-v''sin\theta_t + w''\cos\theta_t\right)^2 + GJ\phi'^2 + F_c v'^2 + F_c w'^2 \right\} dx \qquad (1)$$

where EA, EI_y, EI_z and GJ are the axial, lead-lagging, flapping and torsional stiffness, respectively. The term F_c is the centrifugal effect and is a function of the mass (m) and the blade rotational speed (Ω):

$$F_c = \int_x^R \Omega^2 m x dx \tag{2}$$

To obtain the kinetic energy expression, the approach presented by Magari et al. (1988) is also used here.

$$T = \frac{1}{2}\int_0^R \left\{ \iint_A (\rho d\eta d\zeta) \left(\frac{d\vec{r}}{dt} \cdot \frac{d\vec{r}}{dt} \right) \right\} dx \tag{3}$$

The velocity of an arbitrary point in the blade cross-sections is given by:

$$\frac{d\vec{r}}{dt} = \vec{\omega} \times \vec{r} + \dot{\vec{r}} \tag{4}$$

where:

$$\vec{\omega} = \Omega \vec{k}; \vec{r} = x_1 \vec{i} + y_1 \vec{j} + z_1 \vec{k} \tag{5}$$

The coordinates (x_1, y_1, z_1) of an arbitrary point in the deformed blade cross-section are the same as shown by Marques (1993). The kinetic energy is obtained by substituting the Eq. (4) in the Eq. (3) and calculating the double integrals for the blade cross-section areas. The resulting expressions are far too long, so for the sake of brevity they have been withdrawn and the reader must refer to Marques (1993) for the respective expression.

2.2. Aerodynamic Loading

The steady aerodynamic approach was adopted to yield the expressions of lift (L), drag (D) and aerodynamic moment (M) in the hovering flight condition. Some simplifications were adopted. The first one is neglecting the induced velocity, which yields a free airflow velocity parallel to the y-axis. The small displacement consideration results in the assumption that the blade cross-section remains parallel to the yz plane. There is no coincidence between mass and elastic axes, but the aerodynamic center is taken at the same point of the elastic axis and cross-section intersection. The profile NACA 0015 was assumed; therefore the aerodynamic and the pressure center of the blade cross-section are the same.

A blade element of dx length was taken and the corresponding load element was calculated. Considering that the blade elastic displacements in the free air flow and supposing an operational region of the blade angle of attack, an expression representing the aerodynamic loading results as follows:

$$\begin{bmatrix} D \\ L \\ M \end{bmatrix} = \frac{1}{2}\rho_{ar}\, c \begin{bmatrix} C_{D\alpha} \\ C_{L\alpha} \\ C_{L\alpha} e \end{bmatrix} \int_x^R (\theta_P + \Theta_0 + \theta_t + \phi) \left\{ [\dot{u} - \Omega v]^2 + [\dot{v} + \Omega (x + u)]^2 + \dot{w}^2 \right\} dx \tag{6}$$

where, e is the offset between elastic and mass axis; ρ_{ar} is the air mass density; c is the blade cross-section chord; θ_P is the command pitch angle; Θ_0 is the nominal value of pitch angle in the operational region (10° in this work).

2.3. Piezoeletric Actuation

Piezoelectric materials are those with the ability to generate mechanical displacements due to the application of electrical charge and vice-versa. That electro-mechanical coupling has been more recently utilized in favor of the smart structures concept (Crawley, 1994). Intense loads at high frequencies allow the use of the new piezoelectric actuator technology to control of structures, serving as a motivation to aeroelastic control practices.

For piezoelectric materials the constitutive equations are coupled (Premount, 1997):

$$\begin{aligned} \varepsilon &= (1/E)\sigma + dE_l \\ D^* &= d\sigma + \kappa E_l \end{aligned} \tag{7}$$

where, ε is the strain, E is the Young's modulus (at constant electric field), σ is the stress, d is the piezoelectric constant, E_l is the electric filed, D^* is the dielectric displacement, and κ is the permittivity under constant stress. Piezoelectric

constants are related to the polarization and strain directions. Therefore, d_{31} is normally assumed as the piezoelectric constant for the case of electric field applied perpendicular to the plane of the associated mechanical strain.

The piezoelectric actuators in the form of strips can be bonded on the structure, and that geometrical arrangement is such that d_{31} dominates the design and the useful direction of expansion is normal to that of the electric field. Considering a beam-like smart structure, piezoelectric strips (with thickness h_p) can be used as actuators by controlling the voltage V applied to the electrodes, creating a constant electric field $E_l = V / h_p$.

The equilibrium equation of a beam is given by:

$$m\ddot{w} = -\frac{d^2 M}{dx^2} \tag{8}$$

where m is the beam mass per unit length, w is the beam vertical displacement and M is the bending moment.

According to the Euler-Bernoulli assumption, the axial deformation and curvature are related by:

$$\varepsilon = -z \, {d^2 w}/{dx^2} \tag{9}$$

where z is the distance to the neutral axis.

The bending moment is given by:

$$M = -\int_A \sigma z dA = EI \frac{d^2 w}{dx^2} + E_P d_{31} V b_P h \tag{10}$$

where EI is the bending stiffness referred to the supporting structure and piezoelectric strip, E_p is the piezoelectric Young modulus, V is the applied voltage, b_p is the piezoelectric strip width, and h is the half-value of the beam thickness.

Equation (10) leads to an expression to the concentrated bending moment M_p at the boundaries of the piezoelectric actuator. The piezoelectric moment is, then, given by:

$$M_p = -E_P \, d_{31} \, V \, b_P \, h \tag{11}$$

3. Finite Element Model

The finite element discretization is done in terms of beam elements, with two nodes at each end having six degrees of freedom: displacements in the x, y and z directions, rotation in the xy, xz planes and in the cross-section plane. The nodal displacements (generalized coordinates) form the $\mathbf{q}$ vector and are related with blade displacements through the following equations:

$$\begin{aligned} u &= H_1(x)u_1 + H_2(x)u_2 \\ v &= H_3(x)v_1 + H_4(x)v_1' + H_5(x)v_2 + H_6(x)v_2' \\ w &= H_3(x)w_1 + H_4(x)w_1' + H_5(x)w_2 + H_6(x)w_2' \\ \phi &= H_1(x)\phi_1 + H_2(x)\phi_2 \end{aligned} \tag{12}$$

where $H_1(x)$ through $H_6(x)$ are the shape functions given by third degree Hermitian polynomials, which are the same as in Magari et al. (1988).

Now, the matrices $\mathbf{M}_e$, $\mathbf{G}_e$ and $\mathbf{K}_e$, of each finite element can be obtained. Each coefficient m_{ij}, g_{ij} and k_{ij}, for i,j = 1,2,...n, is obtained by substituting Eq. (12) in the expressions of the strain and kinetic energy. However, these coefficients are not linear in $\mathbf{q}$. Linearization occurs through the assumption of small motions about the equilibrium point (Meirovitch, 1990), what yields the following expressions for the coefficients:

$$m_{ij} = \left.\frac{\partial^2 T}{\partial \ddot{\mathbf{q}}_i \partial \ddot{\mathbf{q}}_j}\right|_{\mathbf{q}=\mathbf{0}} \quad , \quad g_{ij} = \left.\frac{\partial^2 T}{\partial \ddot{\mathbf{q}}_j \partial \mathbf{q}_i}\right|_{\mathbf{q}=\mathbf{0}} - \left.\frac{\partial^2 T}{\partial \ddot{\mathbf{q}}_i \partial \mathbf{q}_j}\right|_{\mathbf{q}=\mathbf{0}} \quad , \quad k_{ij} = \left.\frac{\partial^2 U}{\partial \mathbf{q}_i \partial \mathbf{q}_j}\right|_{\mathbf{q}=\mathbf{0}} - \left.\frac{\partial^2 T}{\partial \mathbf{q}_i \partial \mathbf{q}_j}\right|_{\mathbf{q}=\mathbf{0}} \tag{13}$$

The same procedure is done in order to obtain the loading vector $\mathbf{Q}$. By substituting Eq. (12) in Eq. (6), nonlinear loading expressions are obtained and linearized next. This loading vector $\mathbf{Q}$ is composed by two parts. A first one

depends only of control inputs (voltage, V, to the piezoelectric actuator) and a second one depends only of system generalized coordinates.

The system matrices are formed (Meirovitch, 1990) by superposing each $\mathbf{M}_e$, $\mathbf{G}_e$ and $\mathbf{K}_e$, respectively, and considering the system constraints. The damping effect has been introduced to the model by using the Rayleigh approach (Clough and Penzien, 1975) and a damping factor of $\xi = 0.05$.

The mathematical model obtained results in the following matricial equation of motion:

$$\mathbf{M}\ddot{\mathbf{q}} + (\mathbf{G} + \mathbf{C}_a)\dot{\mathbf{q}} + \mathbf{K}\mathbf{q} = \mathbf{Q}(V, \mathbf{q}, \dot{\mathbf{q}}) \tag{14}$$

4. State Space Representation and Model Reduction

Viewing the applications in control, it is convenient to transform the Eq. (14) into state-space representation. Then, taking the state vector $\mathbf{x}(t) = [\ \mathbf{q}^T\ \ (d\mathbf{q}/dt)^T\ ]^T$, and premultiplying the Eq. (14) by $\mathbf{M}^{-1}$, it follows that:

$$\dot{\mathbf{x}}(t) = \mathbf{A}\mathbf{x}(t) + \mathbf{B}\mathbf{Q} \tag{15}$$

where $\mathbf{A}$ is the state matrix and $\mathbf{B}$ is the input matrix. The loading vector $\mathbf{Q}$, when represented in state-space form can be written as $\mathbf{Q}_1\ \mathbf{x}(t) + \mathbf{Q}_2\ \mathbf{u}(t)$, where $\mathbf{u}(t)$ is the control input vector.

Taking each part of the loading vector and applying in Eq. (15) results:

$$\begin{aligned} \dot{\mathbf{x}}(t) &= \mathbf{A}_1\mathbf{x}(t) + \mathbf{B}_1\mathrm{u}(t) \\ \mathbf{y}(t) &= \mathbf{C}\mathbf{x}(t) \end{aligned} \tag{16}$$

where $\mathbf{A}_1 = \mathbf{A} + \mathbf{B}\ \mathbf{Q}_1$, $\mathbf{B}_1 = \mathbf{B}\ \mathbf{Q}_2$, $\mathbf{y}(t)$ is the output vector and $\mathbf{C}$ is the output matrix.

The high order of original blade model makes it necessary to use a reduction procedure. The technique adopted here is the same as that described by Marques (1993). It uses the original system represented in the for of a transfer function matrix written as a partial fraction expansion:

$$\mathbf{H}(s) = \sum_{j=1}^{2n} \frac{\mathbf{C}\mathbf{h}_{1j}\mathbf{f}_{1j}^T\mathbf{B}_1}{s - \lambda_{1j}} \tag{17}$$

where the $\mathbf{h}_{1j}$, $\mathbf{f}_{1j}$, are the matrix $\mathbf{A}_1$ right and left eigenvectors, respectively, and the λ_{1j} are the matrix $\mathbf{A}_1$ eigenvalues.

Selecting a convenient set of r eigenvalues, which will remain in the Eq. (17), and applying the appropriate transformation, the result is the reduced orthonormal eigenvectors $\mathbf{U}$ and $\mathbf{V}$, which are applied to the Eq. (16) in terms of $\mathbf{x}_r(t) = \mathbf{V}\ \mathbf{x}(t)$. Then, the reduced order model obtained is:

$$\begin{aligned} \dot{\mathbf{x}}_r(t) &= \mathbf{A}_r\mathbf{x}(t) + \mathbf{B}_r\mathbf{u}(t) \\ \mathbf{y}(t) &= \mathbf{C}_r\mathbf{x}(t) + \mathbf{D}_r\mathbf{u}(t) \end{aligned} \tag{18}$$

where, $\mathbf{A}_r = \mathbf{V}\ \mathbf{A}_1\ \mathbf{U}$, $\mathbf{B}_r = \mathbf{V}\ \mathbf{B}_1$, $\mathbf{C}_r = \mathbf{C}\ \mathbf{U}$ and $\mathbf{D}_r$ is given by those eigenvalues of $\mathbf{A}_1$ that were neglected from the system.

4. Control Law Design via Eigenstructure Assignment

The control strategy was idealized for the case of a typical blade pitch control linkage. At a first moment an ideal actuator is placed at the pitch control rod and its action on the blade pitch depends on the measure of displacements or velocities got from some sensors placed along key points of the blade span. Therefore, the idea is to control vibrations on the blade through changes of its pitch angles.

The eigenstructure assignment by output feedback is applied to yield a gain matrix $\mathbf{R}$ that leads to the control system described above. Due to the size of the original system given by the Eq. (16), the control law will be applied to the reduced one.

For output feedback and for the case of a regulator, the control inputs are:

$$\mathbf{u}(t) = -\mathbf{R}\mathbf{y}(t) \tag{19}$$

Substituting the Eq. (19) in the Eq. (18) and working algebraically, one reaches the following closed-loop equation:

$$\dot{\mathbf{x}}_r(t) = \left[\mathbf{A}_r - \mathbf{B}_r\left(\mathbf{I} - \mathbf{R}\mathbf{D}_r\right)^{-1}\mathbf{R}\mathbf{C}_r\right]\mathbf{x}_r(t) \tag{20}$$

For assessment of the matrix **R**, a set of eigenvalues and eigenvectors must be assigned in order to yield the desired time response characteristics of the closed-loop system. Therefore, for each eigenvalue and its respective eigenvector, it must be taken the null space of $[(\mathbf{A}_r - \lambda_j^d\ \mathbf{I})\ \ \mathbf{B}_r]$ (for j=1,2,..,n) that gives another vector, where after its decomposition results in:

$$\left[\mathbf{q}_1^d \quad \mathbf{q}_2^d \quad \dots \quad \mathbf{q}_p^d\right] = \left(\mathbf{I} - \mathbf{R}\mathbf{D}_r\right)^{-1}\mathbf{R}\mathbf{C}_r\left[\mathbf{v}_1^d \quad \mathbf{v}_2^d \quad \dots \quad \mathbf{v}_p^d\right] \tag{21}$$

where p is the number of assigned eigenvalues and $\mathbf{v}^d$ and $\mathbf{q}^d$ result from the null space of $[\ (\mathbf{A}_r - \lambda_j^d\ \mathbf{I})\ \ \mathbf{B}_r\ ]$.

From Eq. (21), one obtains:

$$\mathbf{R} = \left[\mathbf{q}_1^d \quad \mathbf{q}_2^d \quad \dots \quad \mathbf{q}_p^d\right]\left[\mathbf{D}_r\left[\mathbf{q}_1^d \quad \mathbf{q}_2^d \quad \dots \quad \mathbf{q}_p^d\right] + \mathbf{C}_r\left[\mathbf{v}_1^d \quad \mathbf{v}_2^d \quad \dots \quad \mathbf{v}_p^d\right]\right]^+ \tag{22}$$

where $[\ ]^+$ represents the Moore-Penrose pseudo-inverse, since the number of assigned eigenvalues may be different of the number of measured outputs.

5. Results and Discussion

To apply the vibration control strategy a hingeless blade model is assumed. The blade length is 4.09 *m*, and mass of 2.3 *kg*/*m*. The flight condition is hovering with a rotational speed of 360 *rpm*. Other parameters of the problem are: axial stiffness: EA=5.09×10^7 *N*; shifting between CG and elastic axis: e = -0.01013 *m*; torsional stiffness: GJ = 2.28×10^4 *Nm*; flapping stiffness: EI_y = 3.22×10^3 Nm^2; lead-lagging stiffness: EI_z = 1.18×10^5 Nm^2; radius of gyration: k_{m1}=0.008Ns^2; k_{m2}=0.04Ns^2.

The piezoelectric actuator is adopted as the typical PZT (lead zirconate titanate) that presents the following properties: d_{31} = -150 *m/V*; E_p = 50 *GPa*. The piezoelectric strip has been assumed with width of 0.01 *m*, ideally bonded to the main structure of the blade. The actuator length has been taken to coincide with the length of a finite element of the blade model.

The finite element blade model is composed by ten elements all with same length. The actuator loads are considered to be applied at the nodes 3 and 4. The reduced model has been applied considering the first 5 modes with the effect of aerodynamic loading (aeroelastic coupling). It leads to a reduced model with dimension equals to 10. The choice of the frequencies results from the fact that the vibratory behavior of blade is more significant at low frequencies.

The sensors have been placed on node 4, measuring the flapping and lead-lagging velocities on nodes 5, 7, 9 and 11 (blade tip), the torsional gyro ratio on node 7 and the torsional gyro on node 11. These sensors outputs are directly related to the output feedback control strategy. The criteria for choosing those nodes have been based on the fact that at the blade tip, the displacements as well as the velocities are more significant quantities. An increased blade damping is desired to the resulting closed-loop system, and this is achieved by feeding-back velocity quantities. By measuring torsional variables, such as, gyro ratio and gyro on blade tip, one can ensure quick stabilization on torsional motion. This fact is, in principle, important in order to avoid blade stall or even flutter problems.

The next step towards the closed-loop system assessment is to assign the eigenstructure, namely, eigenvalues and eigenvectors. The desired time response, frequencies and damping factors for the closed-loop system were the main factors for the eigenvalues choice. Table 1 shows the assigned (desired) and the achieved eigenvalues for the closed-loop system. The achieved eigenvalues are rigorously identical to the assigned ones.

MODES *(reduced order)*	*Assigned Eigenvalues*	*Achieved Eigenvalues*
1	-4.2654 ± 50.182 *i*	-4.2654 ± 50.182 *i*
2	-9.6309 ± 120.39 *i*	-9.6309 ± 120.39 *i*
3	-14.083 ± 180.55 *i*	-14.083 ± 180.55 *i*
4	-15.042 ± 200.56 *i*	-15.042 ± 200.56 *i*
5	-21.052 ± 300.74 *i*	-21.052 ± 300.74 *i*

Table 1 – Assigned and achieved eigenvalues.

For the eigenvectors, since there is only one control input, it is not possible to modify them.

Next, the simulations of blade motions to initial conditions for open and closed-loop are presented in Figs. (3) to (5). Figure (3) presents the response in lead-lagging motion ($v(t)$)for open and closed-loop cases , respectively. Figures (4) and (5) shows the blade flapping and torsional motion responses for both open and closed-loop cases, respectively. For all the cases, it can be observed effective control actions in reducing vibrations. Overshooting controlled responses can be observed, as well as settling time the order of 0.5 *s*. Actions to improve both controlled responses features shall be considered in further investigations.

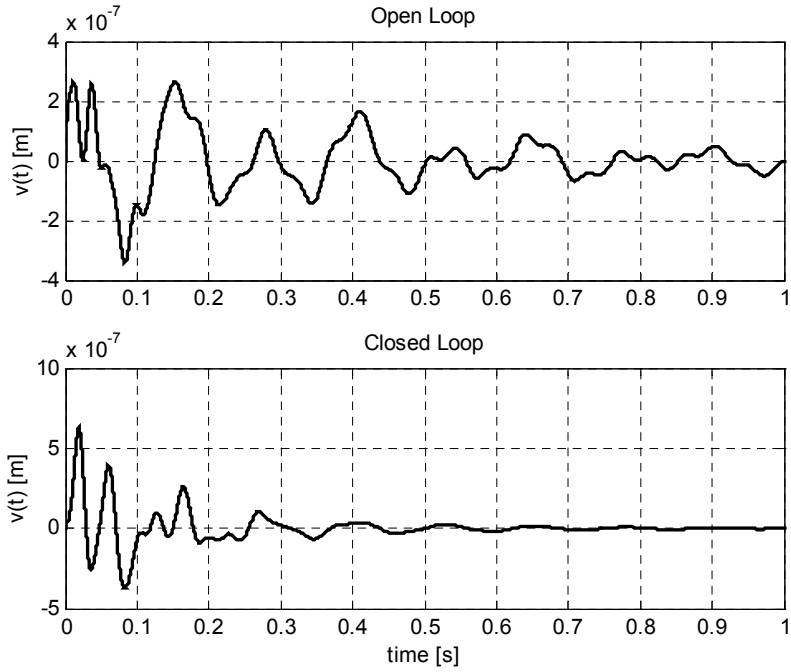

Figure 3 – Blade lead-lagging motion responses for the open and closed-loop cases.

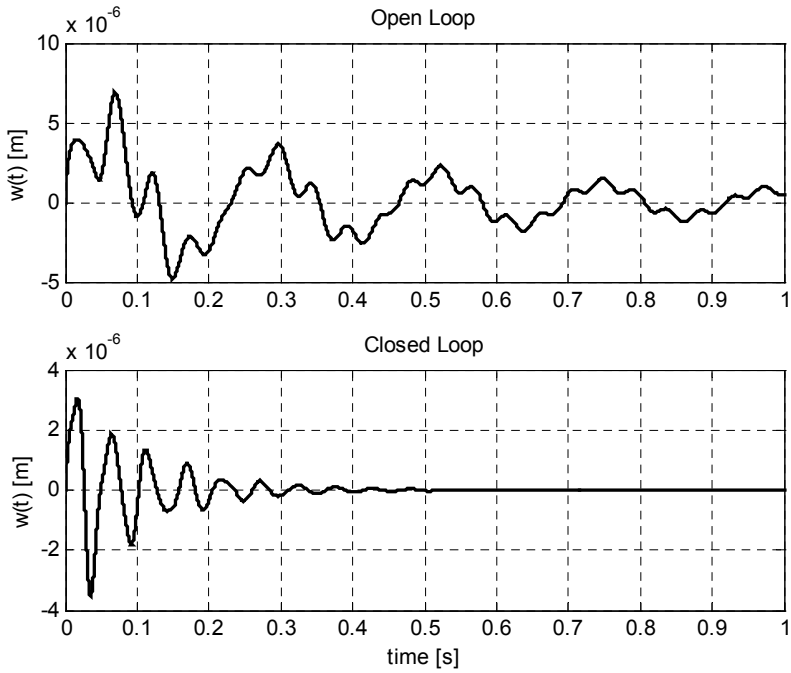

Figure 4– Blade flapping motion responses for the open and closed-loop cases.

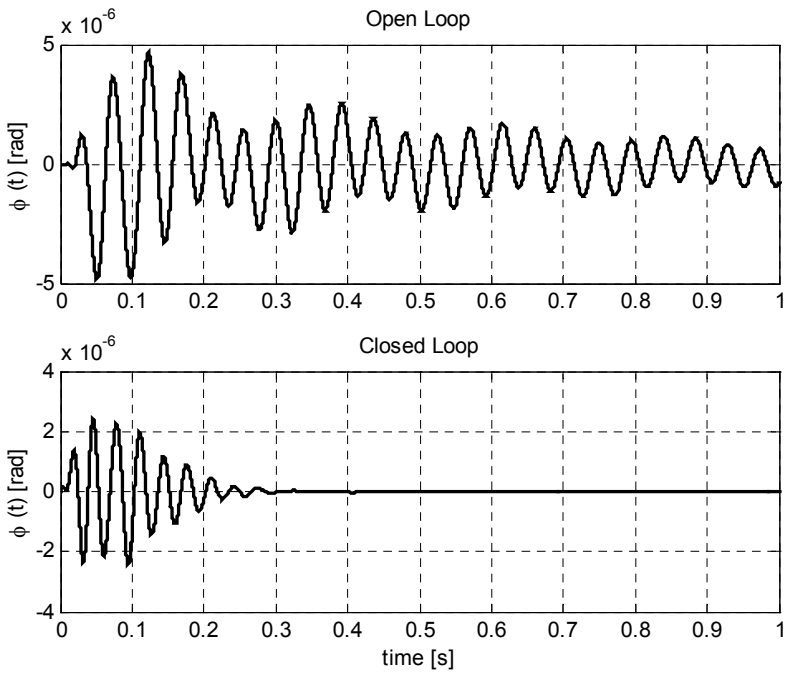

Figure 5 – Blade torsional motion responses for the open and closed-loop cases.

6. Conclusions

This work has presented a study on the application of piezoelectric actuators in the vibration control of helicopter blade. The control law has been assessed with the eigenstructure assignment by output feedback technique. The blade has been modeled by the finite element method. Aerodynamic loading is included to the model to allow aeroelastic coupling. The piezoelectric actuation has been introduced by means of applying voltage-induced moments at specific model nodes. Reduced order model has been produced to speed-up the simulations, as well as to concentrate eigenstructure assignment to the structure modes of interest.

As a form of reducing the vibration on a helicopter blade, the eigenstructure assignment by output feedback shows to be efficient, and a promising alternative for further studies. The technique has affectively led to a control system with eigenvalues (dynamical features) identical to the desired ones. The closed-loop responses have shown good characteristics for both overshoot and settling times. Piezoelectric actuation has proved to be efficient for the case of suppressing helicopter blade vibrations. Further investigations shall concentrate on improving closed-loop responses and on investigating a form of validating the model and the concept of smart blade for practical applications in aeronautical engineering.

7. Acknowledgements

The authors wish to acknowledge the financial support of the Brazilian Research Agency CAPES/CNPq (grant 520356/00-4) and the São Paulo State Research Agency FAPESP (97/13323-8).

8. References

Clough,R.W. and Penzien,J., 1975, "Dynamics of structures", McGraw-Hill, New York, USA.

Crawley, E., 1994, “Intelligent structures for aerospace: a technology overview and assessment”, AIAA Journal, V. 32, pp.1689-1699.

Friedmann, P.P.,1990, “Helicopter rotor dynamics and aeroelasticity: some key ideas an insights”, Vertica, Vol. 14, pp. 101-121.

Loewy, R.G., 1984, “Helicopter vibrations: a technical perspective”, Journal of American Helicopter Society, Vol. 29, pp. 4-30.

Magari, P.J., Shultz, L.A. and Murthy, V.R., 1988, “Dynamics of helicopter rotor blades”, Computer & Structures, Vol. 29, pp. 763-776.

Marques, F.D.,1993, "Analysis and Vibration Control of a Helicopter Rotor Blade"., M.Sc. Dissertation, USP, Brazil, 215 p.

Meirovitch, L., 1990, "Dynamics and control of structures", John Wiley & Sons, New York, USA.

Millott, T.A. and Friedmann, P.P., 1994, “Vibration reduction in hingeless rotors in forward flight using an actively controlled trailing edge flap: implementation an time domain simulation”, Proc. of the 35th

AIAA/ASME/ASCE/AHS/ASC Structures, Structural Dynamics, and materials Conference, Hilton Head, USA, April 21-22, paper AIAA-94-1306-CP.
Nguyen,K. and Chopra,I., 1990, “Application of higher harmonic control to rotors operating at high speed and thrust”, Journal of American Helicopter Society., Vol.35, pp. 78-89.
Nitzsche, F. and Breitbach, E., 1992, “Individual blade control of hinged blades using smart structures”, 18th European Rotorcraft Forum, Avignon, France, Sept. 15-17, pp.E6.1-E6.13.
Nitzsche, F., 1994, “Design efficient helicopter individual blade controllers using smart structures”, Proc. of the 35th AIAA/ASME/ASCE/AHS/ASC Structures, Structural Dynamics, and materials Conference, Hilton Head, USA, April 21-22, paper AIAA-94-1766-CP.
Preumont, A., 1997, "Vibration Control of Active Structures", Kluwer Academic Publishers, Netherlands.
Reichert, G., 1981, “Helicopter vibration control: a survey”, Vertica, Vol. 5, pp.1-20.
Straub, F.K. and Warmbrodt, W., 1985, “The use of active controls to augment rotor/fuselage stability”, Journal of American Helicopter Society, Vol. 30, pp. 13-22.
Takahashi, M.D. and Friedmann, P.P., 1991, “Helicopter air resonance modeling and suppression using active control“, Journal Guidance, Control and Dynamics, Vol. 14, pp. 1294-1300.

9. Copyright Notice

The authors are the only responsible for the printed material included in this paper.